



# Nanosilica Entrapped Alginate Beads for the Purification of Groundwater Contaminated with Bacteria

Lakshmipriya Ravindran<sup>1,2</sup> · K. Jesitha<sup>1</sup> · P. U. Megha<sup>3</sup> · S. Anilkumar<sup>2</sup> · M. S. Sreekala<sup>1</sup> · P. S. Harikumar<sup>4</sup>

Received: 7 August 2021 / Accepted: 10 November 2021

© The Author(s), under exclusive licence to Springer Nature B.V. 2021

## Abstract

Nowadays the World is facing a scarcity of safe drinking water and the water sector encounters great challenges. The impact of a growing population and the change of climate on water availability and quality; public health and environmental issues related to emerging pollutants are the major challenges that need to be addressed. In drinking water, there may be a chance of having water-related diseases and health issues due to the occurrence of some pathogens. In the present study, we synthesized nanosilica from rice husk and it was encapsulated with sodium alginate beads and tested its efficiency for removal of bacteria from drinking water. These beads are novel since it is fully bio-origin, biodegradable and cost-effective. The isolated nanosilica were characterized spectroscopically and morphologically (FT-IR, XRD, FESEM, and HRTEM). The synthesized beads were characterized by FT-IR, FESEM, and EDX and antibacterial analysis. Using the Petrifilm method and column disinfection experiment, different filler loadings were optimized and found that higher content (1.25 g) of nanosilica reduced bacterial contamination of drinking water. The alginate-nanosilica beads are cost-effective compared to alginate beads incorporated with other nanomaterials. The antibacterial evaluation verified superior antibacterial efficacy against E.coli. The prepared alginate-nanosilica beads can be used in the wastewater treatment industry, as an effective antibacterial agent.

**Keywords** Nanosilica · Alginate · Groundwater · Bactericidal activity

## Highlights

- Nanosilica was extracted from Rice husk, an agro-waste.
- Nanosilica were reinforced in Alginate beads.
- The new environmentally benign beads were efficient in removing bacteria from contaminated groundwater.
- The beads have shown 92% of disinfection efficacy with 20 min of HRT, indicating that the beads can be used more extensively.
- This research can be scaled up to a low-cost water filtration system to assure clean water in contaminated locations.

✉ M. S. Sreekala  
sreekalams@yahoo.co.in

<sup>1</sup> Postgraduate & Research Department of Chemistry, Sree Sankara College, Kalady, Kerala 683574, India

<sup>2</sup> Postgraduate & Research Department of Chemistry, N.S.S Hindu College, 686102 Changanacherry, Kerala, India

<sup>3</sup> Department of Biology, SN College, Chelannur, Kozhikode, Kerala 673616, India

<sup>4</sup> Centre for Water Resources Development and Management, 673571 Kozhikode, Kerala, India

## 1 Introduction

Owing to the increasing demand for drinking water, researchers are facing a challenging task to develop materials that should easily remove the contaminations in drinking water as well it should not make any harm to nature. Both developed and developing countries are facing this serious issue [1]. Every year water-borne diseases kill a large population. Many people in developing countries depend on water resources like rivers, ponds, wells, streams, etc. Due to bacterial contamination, the water turns unsafe to drink [2]. Researchers are focused on the decontamination of water over decades [3]. Many of the scientists are focusing on developing bio sorbents for effectively resolving water-related issues [4]. Y. Orooji, et al. [5] used two distinct methods, such as hydrothermal, co-precipitation-sonication processes and, the very active visible light photocatalysts, silver iodide-graphitic carbon nitride (AgI/g-C<sub>3</sub>N<sub>4</sub>) nanocomposites were synthesized and analyzed. This technique has got a lot of interest since it converts organic pollutants into innocuous inorganic chemicals (such as H<sub>2</sub>O, CO<sub>2</sub>) that don't cause any harmful pollution in the future. The

same group have fabricated another photocatalyst based on  $\text{Gd}_2\text{ZnMnO}_6/\text{ZnO}$  and exhibited as an effective photocatalysts for the breakdown of dye contaminants [6]. P. Mehdi-zadeh et al. [7] fabricated  $\text{TbFeO}_3$  ceramic nanostructures as photocatalyst for the adsorbing organic dyes in water. Treatment of water that included Methyl orange, Acid Black 1, Acid Blue 92 and Acid Brown 214 was carried out using fabricated nanomaterials. Additional research looked at the effects of contamination level and pH on the degrading efficiency of contaminant-containing solutions. In an acidic environment,  $\text{TbFeO}_3$  nanostructures exhibit greater photocatalytic properties while also exhibiting reduced pollution level.

Karimi-Maleh et al. [8] fabricated chitosan hydrogel beads incorporating 1-butyl-3-methylimidazolium bromide (BmImBr). From the results, they observed that the CS bead was successfully impregnated with the BmImBr. With a removal percentage of 86% in less than half an hour, the produced beads are highly effective for removing methylene blue (MB) from water. The removal percentage increased with increasing sorbent dose and increasing pH of the solution. To catalyze the deterioration of an organic dye, two tri-metal layered double hydroxides (LDH- (FeCuMg and CrCuMg) were used as sonophotocatalysts [9]. To clean dye-contaminated wastewater, scientists are turning to sonocatalysis with the help of an appropriate catalyst. The compounds that have been produced are not only capable of decolorizing textile wastewaters by sonophotocatalysis, but they are also capable of inactivating harmful bacteria present in the wastewater before being released into the environment. This capacity increases the reusability potential of treated effluent, allowing it to be utilized in industrial processes and other beneficial uses in the future.

One of the major water quality concerns across the world is caused by pathogen contamination [10]. In the majority of water bodies in India, pathogen contamination is a serious threat [11, 12]. The Central Pollution Control Board (CPCB) has released a database of water quality data that shows significant organic and microbiological infestation in several groundwater bodies. [13]. Untreated household and industrial wastewater discharged into water bodies from metropolitan areas may be a major source of pollution [14, 15]. If the receiving water bodies do not have enough water flow for dilution, oxygen demand and bacterial pollution may increase. Studies have reported water contamination due to industrial pollution in several regions of Kochi, Palakkad, Kollam, Kozhikode, and Kannur districts of Kerala. In Kerala, for drinking purposes almost 60% of the people depend on groundwater; but most of the open wells are under the threat of bacterial contamination. The open nature of wells, the use of buckets and ropes to collect water, cooking wastes, and drainage systems below 7 m from wells are all important contributors to microbiological pollution.

Nanoparticles may be used for wastewater management and have a wide range of uses in aquatic systems, both ex-situ and in-situ. [16–18]. Because of its stability and cost-effectiveness, silica nanostructures have attracted interest in water treatment methods [19–21]. Due to the availability of natural resources and increasing demand for recycling agro waste, the utilization of biopolymers is important [22–24]. The biopolymer derivatives for adsorption studies are low-cost and environmentally benign. Activated carbon is the commonly used adsorbent are which was found to be expensive and less efficient. The increasing numbers of publications in the field of biopolymers are true evidence showing its importance worldwide. But the studies investigating the formation and manipulation of biopolymers in wastewater treatments are being reported only in fewer numbers. Modification of the biopolymer to aid in water purification can have immense implications on the development of water treatment technologies. A large number of multipurpose porous membranes and nanocomposites can be fabricated by integrating nanomaterials that outperform traditional materials. These unique materials allow the retention of particles and pollutant prevention [25].

Among the biopolymers, Alginate is found to be of great interest. It can be transformed into beads and films and is ideal for adsorption studies. Also, it is hydrophilic, contains a large number of functional groups, and is flexible. “Alginate is a linear polysaccharide comprised of (1,4)-linked  $\beta$ -D-mannuronate (M) and  $\alpha$ -L-guluronate (G) residues and is extracted from seaweeds”. Polysaccharides have several benefits, including being compostable, safe, easy to handle, and biocompatible.

Shim et al. [26] investigated the effectiveness of alginate beads reinforced with silica and immobilized bacteria for water remediation. Heavy metal elimination was shown to be more effective with alginate beads containing silica than with zeolite beads. Baek et al. [27] developed zinc oxide entrapped alginate beads for the remediation of antibiotic-resistant bacteria. They studied the mechanism for antibacterial property and reusability of the synthesized beads. The adsorption of divalent metal ions can be done by using alginate beads. This adsorption efficiency is due to the -COOH and -OH groups present in the corresponding biopolymer via the ion exchange process [28, 29]. Ocinski et al. [30] developed alginate beads incorporated with water treatment residuals (WTR) for treating water containing arsenic. Effective disinfection properties were exhibited by silver incorporated alginate beads and these beads showed effectiveness for E.coli remediation [31]. Novel alginate bead composites were fabricated by the integration of  $\text{MnO}_2$  nanoparticles [32]. They have checked the kinetics of the sorption mechanism, reusability, and adsorption efficiency.

Factors like population growth, urbanization, unavailability of water due to weather changes, and expanding areas of

water scarcity increase pressure on existing drinking-water resources, and there exist an urge to figure out an alternative method for the supply of drinking water. Economically and practically, potable reuse and disinfection methods can maintain the sustainability of drinking-water supplies [33]. The major drawbacks associated with conventional disinfectants are the production of carcinogenic by-products. These carcinogens are generated by the reaction between the oxidants present in disinfectants and natural organic matter. This paper reports on the extraction of nanosilica from the husk of rice followed by entrapping into alginate beads for water treatment. We chose alginate because it is readily available and nontoxic as an encapsulation medium. Porous columns of alginate-nanosilica beads were packed to pass bacterially contaminated water. The impact of hydraulic retention time (HRT) in the column is investigated. The characterizations of extracted nanosilica were done by FT-IR, XRD, FESEM, and HRTEM. The bactericidal ability of synthesized alginate entrapped nanosilica beads has been utilized in the purification of water.

## 2 Materials and Methods

### 2.1 Materials

Rice husk was collected from the various of sources in the area (rice mill, Kalady, Kerala, India). Sodium alginate, Calcium chloride, Sodium hydroxide, and Hydrochloric acid, of AR grades were procured from Merck India.

### 2.2 Methods

#### 2.2.1 Extraction of Nanosilica Derived from Rice Husk

Rice husk is the raw material and was obtained from the rice mill at Kalady, Ernakulam, Kerala. Analytical grade reagents were used and their solutions were prepared in distilled deionized water. To get rid of impurities like sand and dust, the rice husk was thoroughly cleansed. Later calcination was done to obtain the ash. A programmable muffle furnace was set at 650 °C and the husk was calcinated for 2 h. All the organic compounds were degraded at 500 °C and a large amount of ash with high silica content was obtained at 650 °C. To the above-calcinated rice husk, ash added 1.5 M NaOH solution. Stirred constantly for three hours with the help of a magnetic stirrer at 80 °C and filtered. Continued the filtration till the filtrate was clear. Then concentrated hydrochloric acid was added to the above filtrate dropwise by constant stirring using a magnetic stirrer till silica gel (transparent white silica sol) formed. The silica gel was centrifuged by washing many times with deionized water and then dried in the oven at 50 °C for 48 h. Finally, after the

calcination of the dried powder (723 K for 2 h), pure silica powder was obtained.

The overall process is indicated in Fig. 1.

#### 2.2.2 Synthesis of Calcium Alginate Beads for Encapsulation of Nano Silica

In 100mL deionized water, sodium alginate (3 g) was stirred at 50 °C. Complete dissolution was achieved when the alginate–water mixture was magnetically stirred for 30 min. The above alginate solution was gradually incorporated with the 0.5 g/0.75 g/1 g/1.25 g of nano silica. To ensure maximum entrapment, the alginate solution and nanosilica mixture were continuously stirred with a glass rod. Then the solution was sonicated for half an hour at room temperature for complete dissolution. The resultant viscous mixture was quickly dropped into a 0.73% deoxygenated cooled aqueous solution of CaCl<sub>2</sub> and beads were formed. After washing with deoxygenated water the remaining nanosilica which is not entrapped was accounted for by measuring them. Out of a total of 3 g, the average amount leftover was found to be 0.0019 g, which corresponded to an error of 0.19%. In the deoxygenated CaCl<sub>2</sub> solution the gel beads were retained. Hardening takes 9 h, after which it is rinsed with deionized water. An optimal diffusion of substrates into and out of the prepared beads was obtained by hardening for a minimum of 6 h.

### 2.3 Characterisation of Nanosilica and Nanosilica Entrapped Alginate Beads

#### 2.3.1 Fourier Transform-Infrared Spectroscopy

Make use of PERKIN ELMER ATR infrared spectrometer, Fourier Transform Infrared Spectroscopy of nanosilica and nano silica entrapped Ca-alginate beads was observed between 400 and 4000 cm<sup>-1</sup>. Nanosilica powder was taken by mixing with KBr and pellets were made to take the FT-IR spectra. The solution of the alginate-silica mixture was dropped directly onto the diamond to record the IR spectrum.

#### 2.3.2 X-ray Diffraction Analysis (XRD)

The diffraction pattern of the nanosilica was investigated on Bruker AXS D8 Advance with an operating voltage of 45 kV, a wavelength of 1.541 Å, Cu K $\alpha$  radiation with an angle range 5°–80° (2 $\theta$  angle range) and a current of 35 mA.

#### 2.3.3 Field Emission Scanning Electron Microscopy (FESEM)

Hitachi SU6600 Variable Pressure Field Emission Scanning Electron Microscope was utilized to take the morphology of

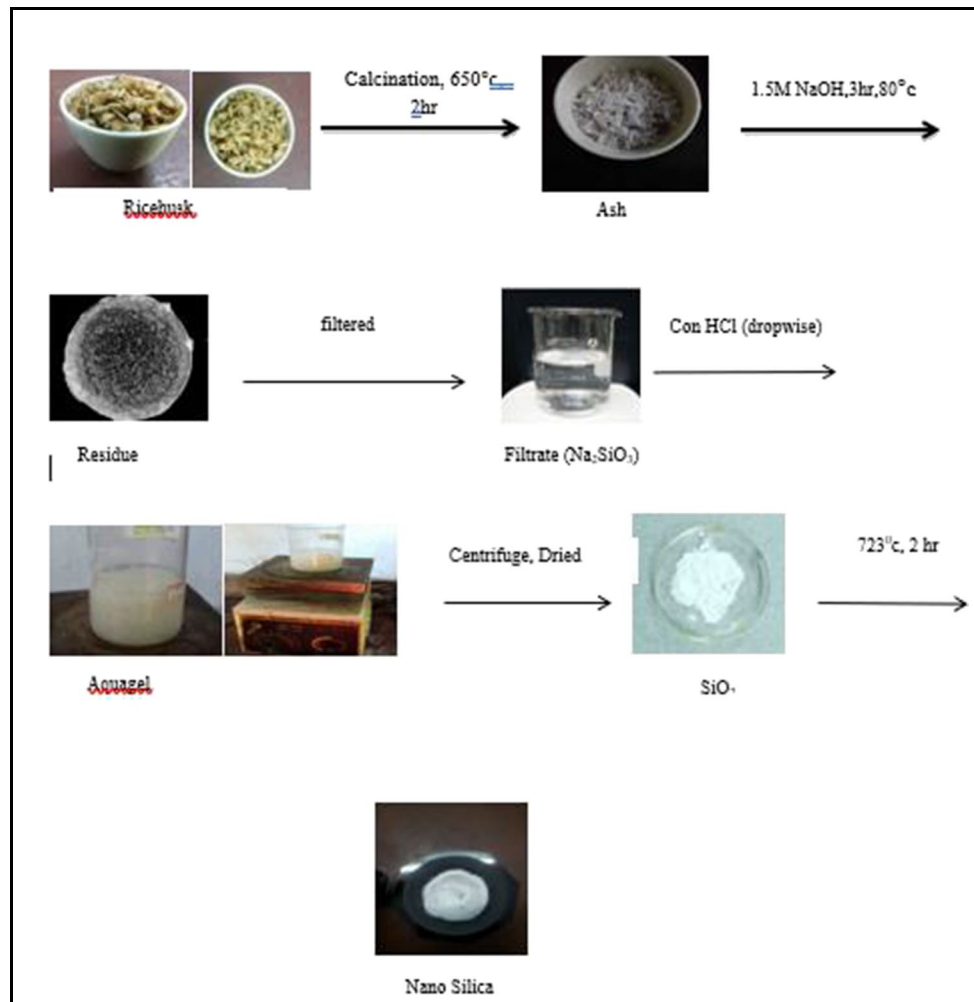


Fig. 1 Schematic representation of the extraction of nanosilica from rice husk

samples (nanosilica and nano silica entrapped Ca-alginate beads) were analyzed at an acceleration voltage of 30 kV and Probe current of 1pA~200nA. Gold sputtering was done on each sample to avoid charging.

### 2.3.4 Transmission Electron Microscopy (TEM)

A High-Resolution Transmission Electron Microscope, JEM-2100 HRTEM was used to obtain the transmission electron micrographs of nanosilica. On a copper grid with a carbon film coating, a dilute suspension of nanosilica was dropped, dried up, and analyzed.

### 2.3.5 Antibacterial Tests

Before the antibacterial assay, the nano-silica powder was disinfected using UV irradiation at room temperature for 12 h. The antibacterial activity of nano-silica powder was further investigated using the agar well diffusion technique

as per the procedure of Valga et al. [34]. Using aseptic techniques, a single pure colony of E.coli was transferred into 10 ml of nutrient broth and was placed in an incubator at 37 °C for overnight incubation. Sterile MHA plates were prepared and the bacterial inoculum of E. coli was uniformly swabbed in each plate. Test samples of different volumes were added to the wells over the agar plates. The samples were incubated at 37 °C for 18 h, which was enough time for the bacteria to proliferate. After incubation, the diameter of inhibitory zones formed around each well was measured in cm and recorded. Three different dilutions of nano-silica beads were used in the study, viz., 25 µl, 50 µl, and 100 µl. Along with the nano-silica beads, ethanol and ampicillin control were kept for E.coli.

### 2.3.6 Column Disinfection Experiment

The quantification of antibacterial efficiency of nano-silica entrapped alginate beads was carried out using a column

experiment. The suspension of E.coli was initially sifted via a densely packed column with alginate beads entrapped with nano-silica. At 37 °C, an E.coli culture was produced in Luria-Bertani broth and sampled at the mid-exponential growth phase. Further, the harvested culture was washed using the centrifugation method, and 10 mM phosphate buffer of 7.4 pH was used to re-disperse the E.coli bacteria. The column with a diameter of 1.8 cm, length of 16 cm, and apparent volume of 30.5 ml was packed with the beads. The flow rates were controlled and adjusted to maintain an HRT (hydraulic retention time) of 1, 5, 10, 15, and 20 min respectively. A ten pore volume of buffer solution was added to the column before injecting the E.coli culture to equilibrate the beads. At five separate periods during the experiment, triplicate samples of the effluent were taken for each run. The E. coli samples were taken immediately after they were obtained and were homogeneously plated on agar plates and incubated at 37°C overnight to view visible colonies. Those influent samples which were not passed through the column and prepared as per the E.coli suspension and the effluent from the column which was packed with blank alginate beads were also plated in triplicates.

### 2.3.7 Application of Nanosilica Entrapped Alginate Beads for Remediation of Bacteria

An antibacterial study of silica nanoparticles derived from rice husk was attempted against gram-negative bacteria E-coli. 3 M Petrifilm method was particularly chosen for the study. The effectiveness of the 3 M Petrifilm Aerobic Count Plate has been compared to normal plating methods in several investigations. According to the findings, the 3 M Petrifilm method was similar to the normal plating methodology and hence may be utilized as an alternate process for counting test organisms in AOAC Methods [35].

A pipette was used to put 1ml of sample onto the center of the plate in the technique. A spreader was used to distribute the sample uniformly over the media surface. Plates were incubated for 24 h at 37 °C. The number of blue colonies (E. coli) and red colonies producing gas was enumerated, Colony-forming units (CFUs)/100 ml water were calculated. For the antibacterial study utilizing silica nanoparticles, a contaminated water sample with high content of E-Coli from an open well at Kalady, Ernakulam, Kerala was selected. The selected water sample was treated with nanosilica (0.5 g, 0.75 g, 1.0 g, 1.25 g) entrapped calcium-alginate beads.

## 3 Results and Discussions

### 3.1 Dry Weight% and Yield Percentage of Nanosilica

A specific amount of rice husk at the muffle furnace was charred at 650 °C for 2 h. Using digital microbalance, the

obtained ash was pre-weighed. The dry weight% of rice husk ash (RHA) was computed with the following formula:

$$\text{Dry weight percentage} = \frac{(\text{Weight of the ash in grams})}{(\text{Weight of rice husk in grams})} * 100$$

$$\begin{aligned} \text{Rice husk (RH)} &= \frac{2.7083}{25.9034} * 100 \\ &= 10.4553 \% \end{aligned}$$

Yield percentage of nanosilica from (RHA) can be determined by the following relation.

$$\text{Yield percentage} = \frac{(\text{Amount of silica nanoparticles synthesized in grams})}{(\text{Amount of rice husk ash used in grams})} * 100$$

$$\begin{aligned} \text{Si}_{(\text{RHA})} &= \frac{1.6676}{2.7083} * 100 \\ &= 61.5\% \end{aligned}$$

The yield percentage of rice husk-derived nanosilica was found to be 61.5%.

### 3.2 Characteristics of Synthesized Nanosilica and Nanosilica Entrapped Alginate Beads

#### 3.2.1 Formation of Alginate Beads

The beads prepared were found to be globular in shape (Fig. 2) with a diameter of 0.5-1 mm. Calcium alginate beads appeared transparent, colorless, and smooth (Fig. 2) whereas nanosilica entrapped beads appeared white with a rough surface (Fig. 2). Schematic diagram of the formation of nanosilica entrapped calcium alginate beads is illustrated in Fig. 3.

#### 3.2.2 Fourier Transform Infrared Spectroscopy (FT-IR):(Nano Silica)

The bending vibration of O-Si-O was observed from peaks along 465 cm<sup>-1</sup> to 485 cm<sup>-1</sup>. The stretching modes of Si-O-Si belonged to bands from 1090 cm<sup>-1</sup> to 1100 cm<sup>-1</sup> and from 790 cm<sup>-1</sup> to 815 cm<sup>-1</sup> [36]. A band at 1640 cm<sup>-1</sup> corresponded to -OH bending vibrations. The presence of hydroxyl groups on the surface and water which is chemically absorbed can be observed from 3450 cm<sup>-1</sup> to 3640 cm<sup>-1</sup>. The Si-O-Si stretching vibrations were assigned at 1056.2 cm<sup>-1</sup>, confirming the existence of silica groups [37]. FT-IR spectra are given in Fig. 4.

#### 3.2.3 X-ray Diffraction (XRD)

XRD pattern of nanosilica isolated from rice husk (Fig. 5) showed a wide-angle at 2θ = 22° confirmed the formation of nanosilica from rice husk. This unique broad peak at 2θ = 22° indicated the presence of silica

**Fig. 2** A) Calcium-alginate beads B) Nanosilica entrapped calcium alginate beads

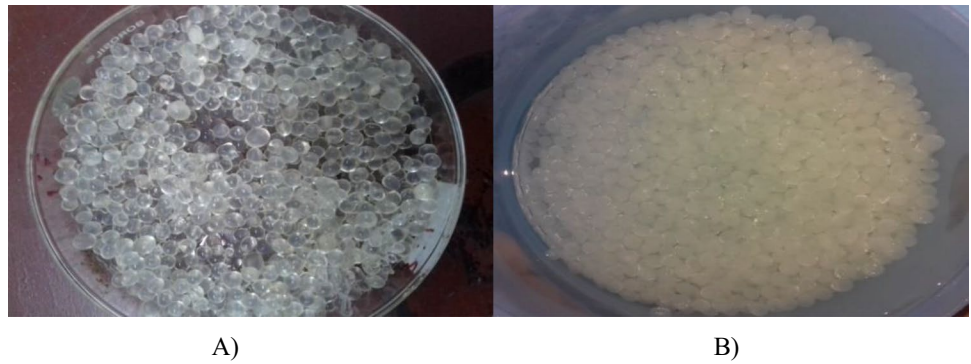


**Fig. 3** Schematic representation of the formation of nanosilica entrapped calcium alginate beads

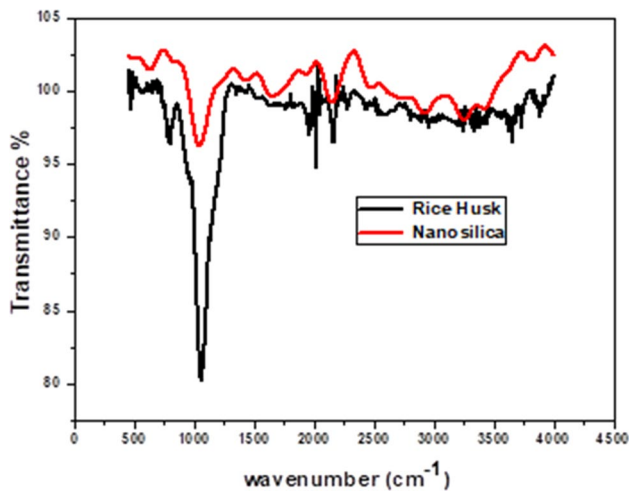
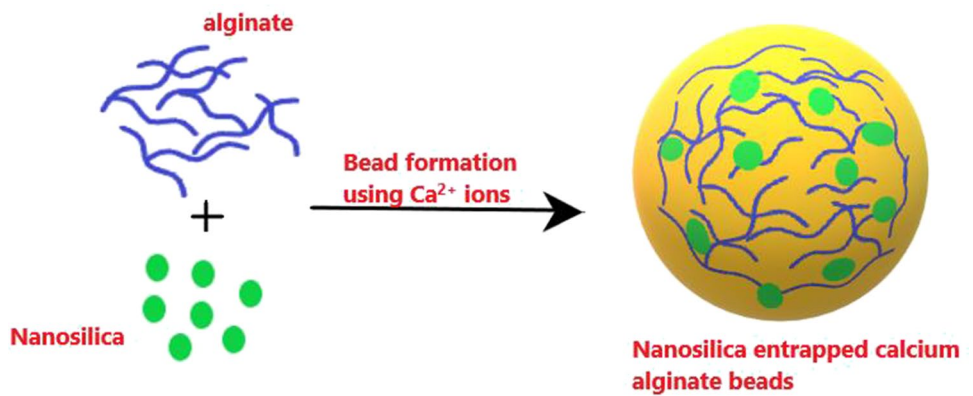


**Fig. 4** FT-IR spectra of rice husk (RHA), nanosilica obtained from rice husk (R)

in the amorphous form[38–40]. If the peak was sharp then the silica obtained should be crystalline. The pure nano silica, on the other hand, was sintered at 1373 K to reach the crystalline phase and quantify the crystallite size.

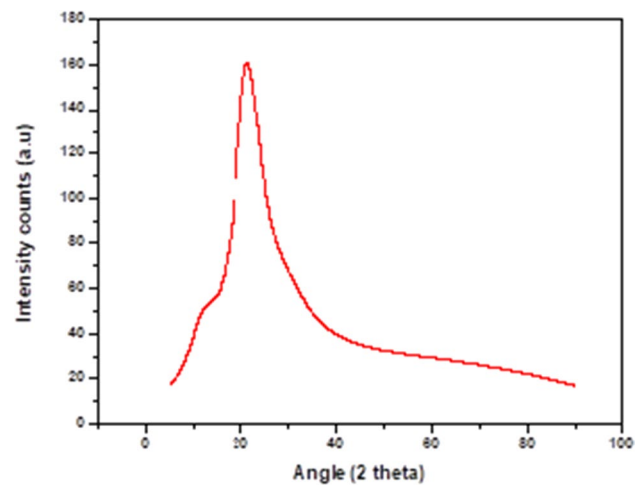


**Fig. 5** XRD curve of nanosilica from rice husk

### 3.2.4 Field Emission Scanning Electron Microscopy (FESEM): Nanosilica

From the SEM analysis (Fig. 6) it was observed that rice husk-derived nano silica exhibited porous structure. The hydrogen bonding between silanol groups on the surface of nanosilica was determined to be the cause of aggregation.

This result is in agreement with other literature reports [41]. It is illustrated in Fig. 7.

### 3.2.5 TEM: Nanosilica

The TEM images and particle size of nanosilica derived from rice husk are shown in Fig. 8. The TEM analysis showed that nanosilica particles formed small clusters following FESEM images. They have an average diameter of about 50 nm. Tan et al. [42] isolated nanosilica from rice husk and used it for iron adsorption. They have got similar results. Many other researchers also got similar TEM images per our results [43–45].

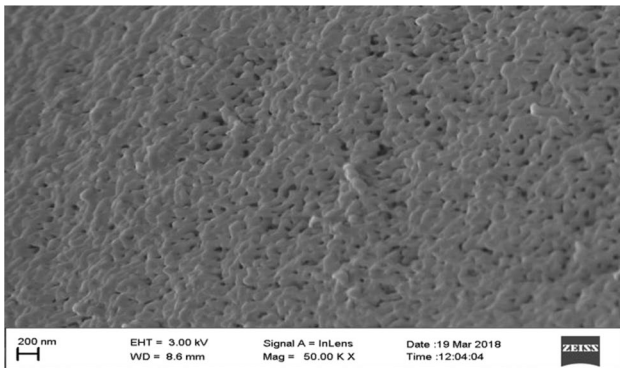


Fig. 6 FESEM image of nano silica obtained from rice husk

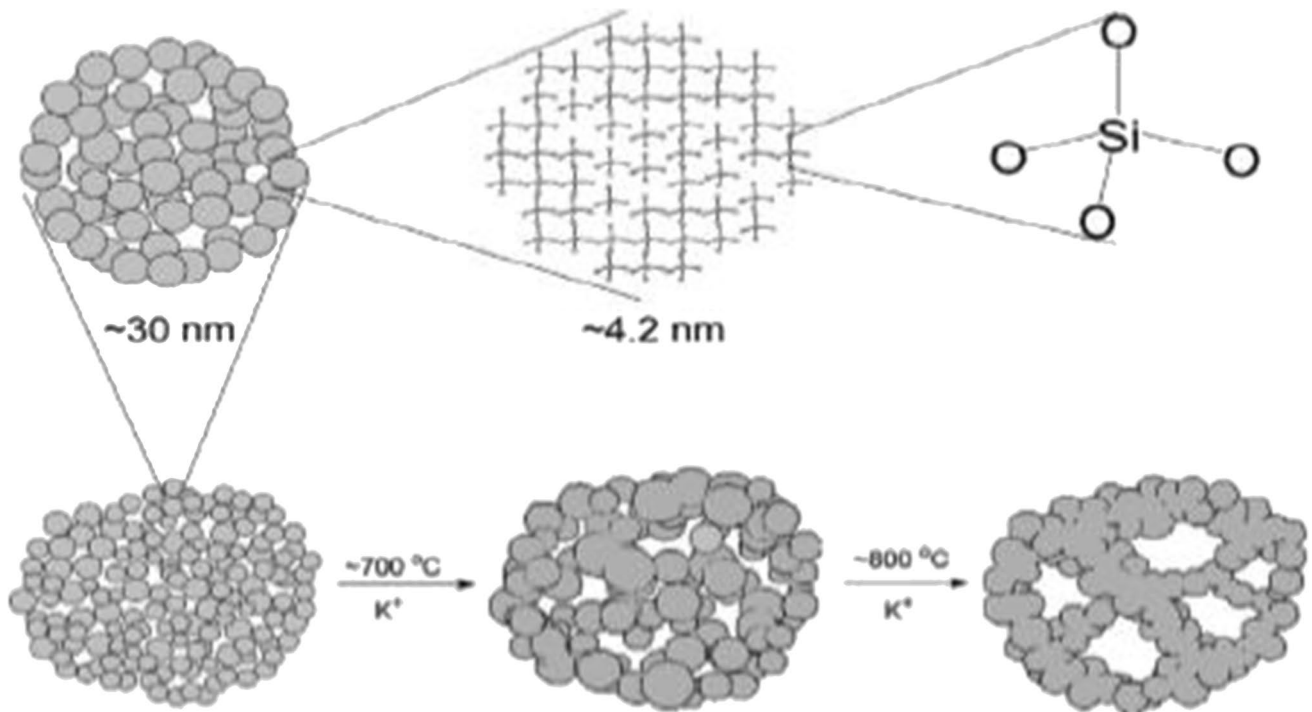


Fig. 7 Schematic representation of nano silica particle prepared from rice husk [41]

### 3.2.6 Fourier Transforms Infrared Spectroscopy (FT-IR) of Nano Silica Entrapped Calcium Alginate Bead

Infrared spectrum of alginate (neat), and reinforced alginate beads (0.5 wt%, 0.75 wt %, 1 wt %, 1.25 wt%) are shown in Fig. 9. The individual functional groups present in alginate beads are not perfectly evident due to the existence of water in excess. The hydrogen-bonded hydroxyl groups found in water are responsible for the large broad peak at  $3320\text{ cm}^{-1}$ . The vibrations such as asymmetric stretching of carboxyl groups found in alginate biopolymer are the reasons for the bands at  $1420\text{ cm}^{-1}$  and  $1610\text{ cm}^{-1}$  [46]. The small peak at  $1090\text{ cm}^{-1}$  is due to the vibration of the carbohydrate ring in alginate. Si-O-Si linkages are the cause for the peak at  $1040\text{ cm}^{-1}$ . These results confirmed the attachment of nanosilica into alginate beads. The Si-O-Si groups will attach to C-O-O- groups present in alginate biopolymer. Previous reports also support our results [43, 47].

### 3.2.7 Field Emission Scanning Electron Microscopy (FESEM) of Calcium Alginate Bead

FESEM image of Calcium alginate beads without entrapped nanosilica particles is indicated in Fig. 10. The results showed that the beads were in spherical shapes [48]. The surface of the spherical spheres was found to be rough. Some researchers have reported similar results [49].

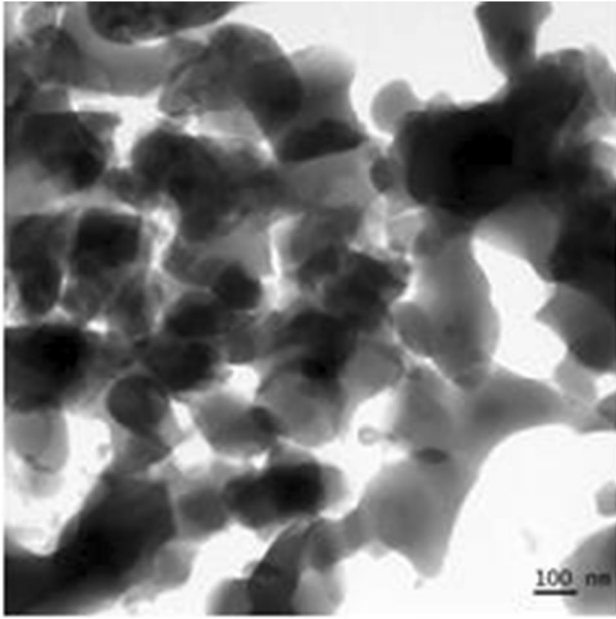


Fig. 8 TEM images of nanosilica

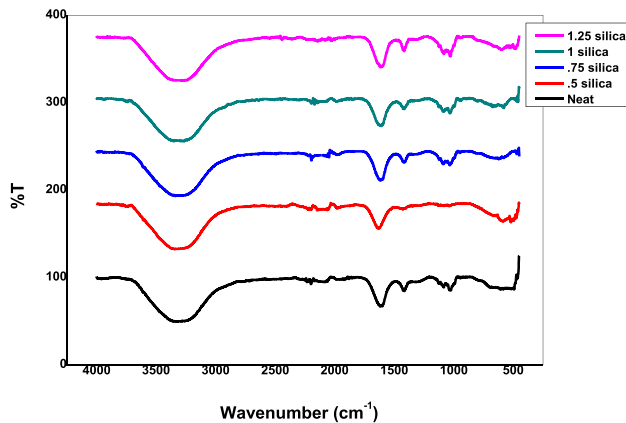


Fig. 9 FT-IR spectra of nanosilica entrapped calcium alginate bead

### 3.2.8 10 Field Emission Scanning Electron Microscopy (FESEM) of Silica Entrapped Calcium Alginate Bead

FESEM analysis was used to analyze the shape of  $\text{SiO}_2$ -alginate beads (1.25), surface properties of produced  $\text{SiO}_2$ -alginate beads, and  $\text{SiO}_2$  dispersion on the beads. Figure 11 gives FESEM images of  $\text{SiO}_2$ -alginate beads. Beads had a consistent plain morphology in FESEM images [43, 50]. (Fig. 11A). The incorporation of nanosilica into the beads improved the surface roughness.  $\text{SiO}_2$  dispersed uniformly throughout the beads are indicated in Fig. 11B. According to these images, nanosilica were found not just on the outside, but also inside the beads, (Fig. 11C). Nanosilica has a diameter of around 30–38 nm.

### 3.2.9 Energy Dispersive X-Ray Spectroscopy (EDS or EDX)

Energy-dispersive X-ray spectroscopy was used to analyze the alginate-nanosilica beads (1.25) further (Fig. 12). The reinforced beads exhibited Si, O, and C signals. The nano-silica entrapment on alginate beads was confirmed by the presence of Si signals. The C and O, on the other hand, come from biopolymers, whereas Ca and Na come from alginate beads. The EDX spectra gave affirmation on the successful reinforcement of nanosilica in the alginate beads.

### 3.2.10 Application of Nanosilica Entrapped Calcium Alginate Beads for the Removal of Bacteria from Drinking Water

**Antibacterial Study of Nanosilica** Antibacterial properties of silica nanoparticles have already been reported. The susceptibility of *E. coli* in the first set of agar well diffusion experiments, the nano-silica powders were put to the test. On *E. coli* plates, there are no inhibition zones (IZs) with 25 and 50  $\mu\text{l}$ , which demonstrates that the nano-silica power should be in larger quantity to affect the organism. Whereas, as shown in Fig. 13., an inhibition zone of 1.3 cm in diameter was obtained for nano-silica power in the agar diffusion well. The nano-silica powder's antibacterial properties are most likely due to the particles' tiny size. This tiny nano-silica has a lot of surface area, so it may have a lot of interaction with the bacterial cells that release a lot of silica. Furthermore, the partial oxidation on the surface of nanosilica was favored by antibacterial tests' aerobic conditions. Antibacterial activities may be enhanced by partially oxidized nano-silica with high silica levels.

The bacterial toxicity property of nano-silica has been observed in various studies[51]. Moreover, the cell wall of *E. coli* is made up of phospholipids, lipopolysaccharides, and transmembrane proteins, as well as layers of peptidoglycan also units of the saccharides abequose, mannose, rhamnose, galactose, and glucose, make up the outer lipopolysaccharide base [52]. The hydroxyl groups of nano-silica aid hydron bonding with saccharides of lipopolysaccharides and the other groups present in *E. coli* resulting in the destabilization of peptidoglycan. Our finding of the antibacterial efficiency of nano-silica is supported by similar studies [53–57]. Silica nanoparticles can interact and kill the bacteria by attachment with its outer wall. Nanosilica connects with the bacterial membrane through hydrogen bonds formed between silanol groups and the functional groups of the bacterial wall. These bonds destabilize the peptidoglycan (bacterial wall) and kill the bacteria [52]. The results of this study also proved that the nanoparticles exhibited good bactericidal activities against *E. coli* bacteria. Moreover, because the silica NPs do not get buried inside the bacterial cells, immobilization



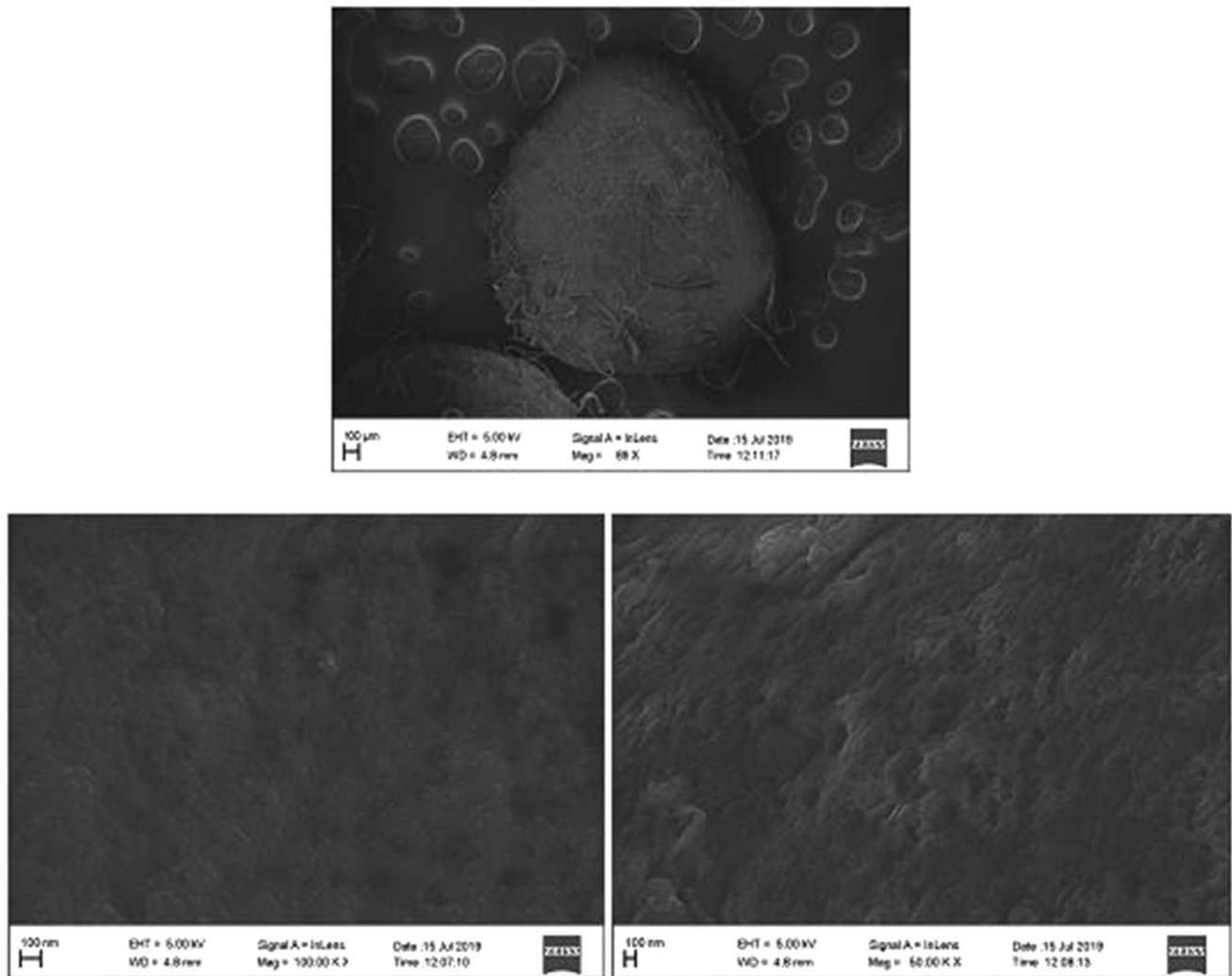


**Fig. 10** FESEM images of calcium alginate beads without the entrapped nanosilica

enables contact-mode interaction of silica NPs with a large number of bacterial cells.

**Antibacterial Study of Nanosilica Entrapped Alginate Beads** Antibacterial study of silica nanoparticles derived from rice husk was attempted against gram-negative bacteria *E. coli*. In environmental water samples, *E. coli* indicates the chances of having human pathogens associated with feces. Blue colonies with gas formation were identified as *E. coli*. Petrifilm plates were selected for the study because of their reliability, cost-effectiveness, and ease of use. Petrifilm method can be utilized to detect and enumerate several microorganisms much easier and faster compared to traditional testing methods [58, 59].

The selected water sample (500 mL) with highly infected *E. coli* was treated with calcium alginate beads entrapped

with different concentrations of nanosilica. Results obtained for the antibacterial study treated with calcium alginate beads loaded with different concentrations of nanosilica for a treatment time of 0.5 and 1 h are indicated in Table 1. The total number of colonies of *E. coli* was found to reduce as concentration rises of silica nanoparticles. The study was continued until the bacterial colonies were not detected. Maximum removal of *E. coli* was obtained on the treatment of contaminated water with 1.25 g silica nanoparticle-loaded alginate beads for a treatment time of one hour. Results of treatment of contaminated water with 1.25 g nanosilica entrapped beads are indicated in Fig. 14.

**Column Experiments Using Nano-silica Alginate Beads** Figure 15 represents the results obtained as per the column experiment studies. The notable feature of this work is that the blank beads which were used as a control for the disinfection experiment were capable of eradicating some portion

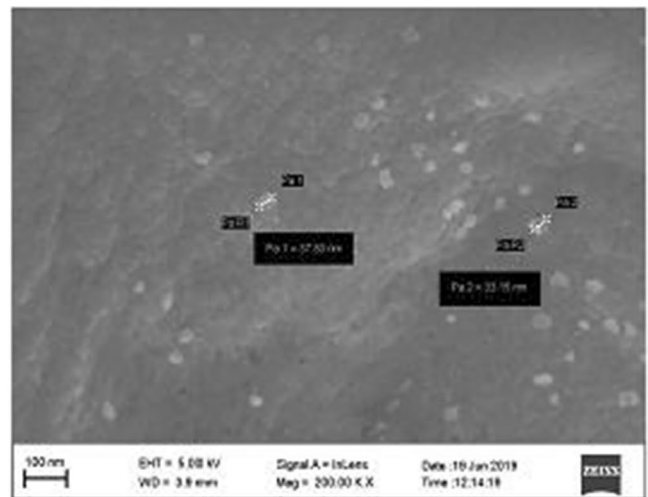
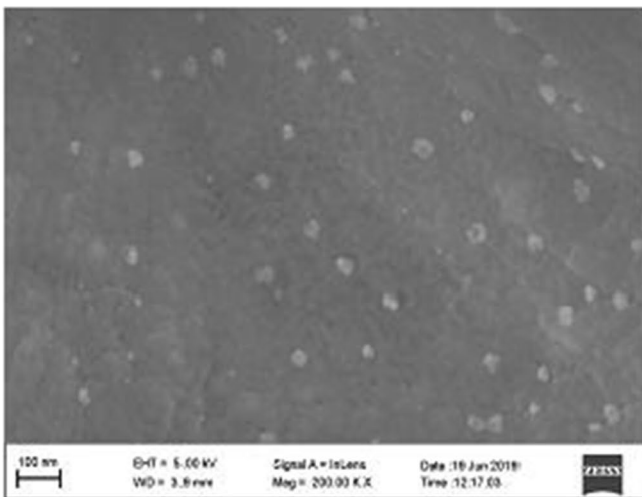
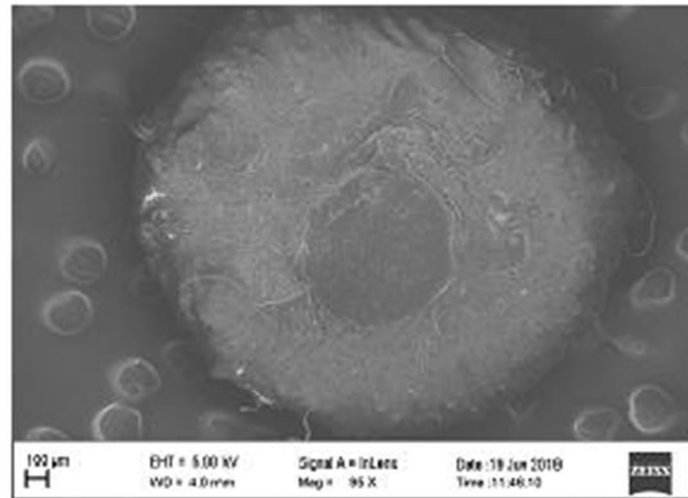
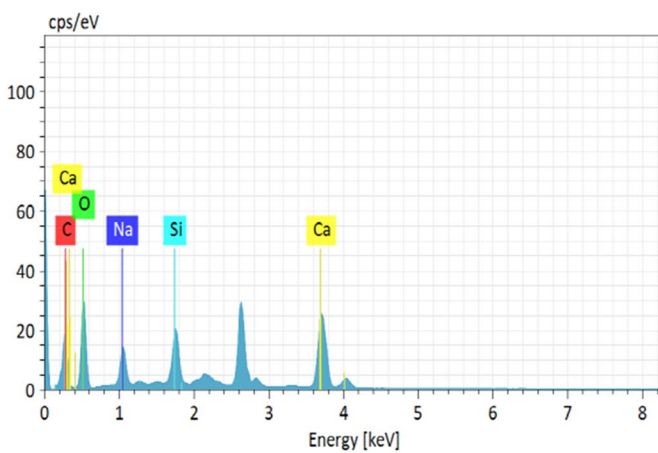


Fig. 11 FESEM images of nanosilica -alginate beads A) morphology of the surface of bead B) nanosilica particles entrapped inside alginate beads C) Dimension of entrapped nanosilica particle



51

Element	At. No.	Netto	Mass [%]	Mass Norm. [%]	Atom [%]	abs. error [%] (1 sigma)	rel. error [%] (1 sigma)
Carbon	6	31382	26.14	30.55	40.75	3.23	12.35
Oxygen	8	57050	41.30	48.26	48.34	4.85	11.74
Sodium	11	25980	5.08	5.94	4.14	0.36	7.01
Silicon	14	43191	3.38	3.95	2.25	0.17	5.05
Calcium	20	74643	9.67	11.29	4.52	0.31	3.20
		Sum	85.58	100.00	100.00		

Fig. 12 Energy Dispersive X-Ray Spectroscopy (EDS or EDX) of nanosilica -alginate beads



**Fig. 13** Antibacterial activity of nanosilica powder

**Table 1** Results of antibacterial study utilizing nanosilica entrapped alginate beads

Concentration of silica nanoparticle entrapped in bead	Bacterial count CFU/100 mL	Bacterial count after remediation CFU/100 mL	
	Initial	0.5 h	1 h
Control	TNTC	800	400
0.5 g		700	300
0.75 g		500	200
1.0 g		300	100
1.25 g		200	Not detected

TNTC-Too numerous to count  $\geq 2500$  CFU/100 mL

of the target bacteria. Just by filtration process a removal rate of 1%, 11%, 22%, and 35% with a hydraulic retention time (HRT) of 1 min, 5 min, 10 min, 15 min, and 20 min respectively was observed. This removal efficiency of blank beads when compared to the classic filtration theory, was found to be slightly higher. As this theory predicted the percentage of particle separation in water treatment plants using deep-bed filtering, it was apt to understand the notable feature of our study by a slight comparison [60]. The failure of classic filtration theory was attributed to the permeable collectors, as it can allow the passage of porous beads under pressure. Which can indirectly affect the efficiency of the collector particles. Despite this, the removal efficiency of blank beads observed as per this study was not found to be enough when it comes to the treatment of drinking water. An additional

observation was the enlargement of alginate beads observed throughout filtration, which can be one of the reasons for removal efficiency. Many research findings were obtained in a study by Lin et al. [31], where they used alginate beads as a control in point-of-use drinking water disinfection. Both biological activations, as well as physical filtration, were achieved using nano-silica alginate beads. A significantly higher disinfection rate of 92% with an HRT of 20 min was achieved using the fabricated nano-silica beads. However, as per the study, it was observed that the HRT has a very meager effect on disinfection efficiency. This might be the effect of nano-silica, as it can render its action on the target bacteria even after the effluent is plated. Therefore, it is also noted that the retention time inside the column can be relatively insignificant, as long as it is not scanty to allow the release of enough nano-silica particles.

## 4 Conclusions

Contamination has put the quality of potable groundwater in jeopardy, and there is always an ever-increasing urge for pure drinking resources. Rice husk nanosilica was isolated and encased in calcium alginate beads. Nanosilica and entrapped beads were characterized by different methods like FESEM, TEM, XRD, FTIR, etc. The entrapped nanosilica inside beads were utilized for remediation of bacteria in drinking water. To various extents, nano-silica powder was shown to be efficient in eradicating *E. coli*. The columns packed with these nano-silica beads can be used as a viable source for the purification of bacteria from potable water. To be precise 92% of disinfection efficiency was observed with 20 min HRT, indicating the further application of these beads. The study also indicated the moderate release of nano-silica from the beads, which implies a better shelf life for the product without even compromising with the disinfection efficiency. Therefore, this research stresses the importance of boosting the production of such non-metal-based nanomaterials for multiple uses, especially water disinfection. Contaminated water was treated with different concentrations of nanosilica for a different contact treatment time of 0.5 and 1 h. The results showed that the nanosilica at a concentration of 1.25 g had the potential to disinfect contaminated water (500 ml) when treated for one hour. This study can be scaled up to a cost-effective water purification system to ensure pure water in areas of bacterial contamination.

### 4.1 Outlook and Future Perspectives

Nanomaterials can be used in the treatment of contaminated water in several means depending on the structure and morphology. Nanotechnology is emerging as an effective medium for the treatment of wastewater commercially

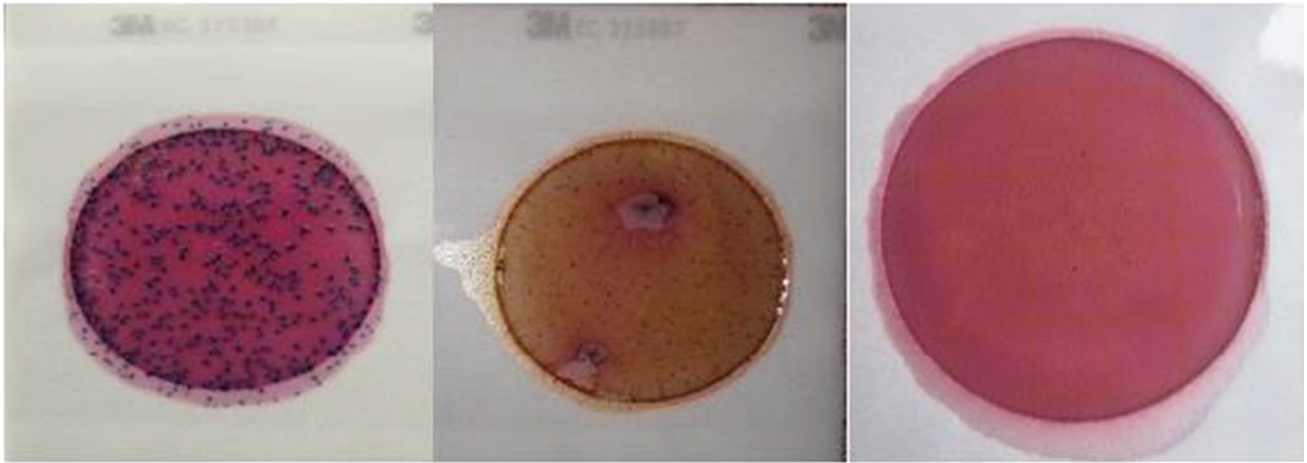
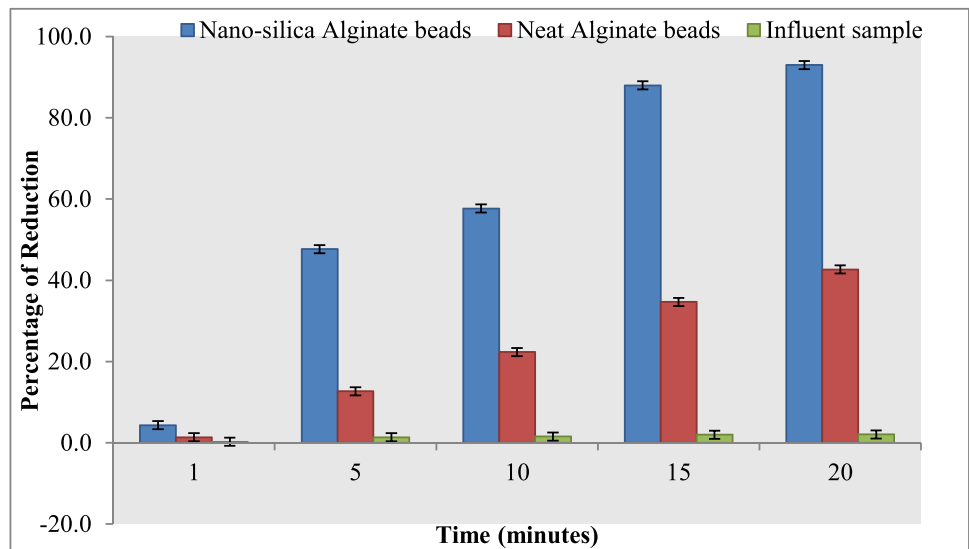


**Fig. 14** Results of treatment of contaminated water with 1.25 g nanosilica entrapped beads **A**) Control (Contaminated water) **B**) Water after treatment with 1.25 g nanosilica for 0.5 h **C**) Water after treatment with 1.25 g nanosilica for 1 h

**Fig. 15** Percentage reduction in *E.coli* per ml sample plated



and nowadays accepted globally. The mechanism of water treatment by nanotechnology consists of adsorption, catalysis, photocatalysis etc. There are many States in India facing challenges of drinking contamination, scarcity of pure drinking water and related health issues. Even 80% of the open wells of Kerala, a Southern State of India are reported to be contaminated with coliform bacteria. Cost effective treatment especially availability of Nanomaterial which can remove bacteria will be helping millions of people all over the world affected with water borne diseases. The present study we hope that, will once developed as water filter can solve many of the water related health issues globally.

One of the major challenges is to ascertain the intermediate composition of the materials if formed any and to remove those materials. Second challenge is related to the reuse of the materials and the determination of its

efficiency while reusing the material. The disposal is also a challenge. We may focus on safe disposal of the product developed and will do a study on the environmental fate and toxicity if any of the material. Cost effective ratio of the technique is very important. The method developed can be popularised in rural areas only if the filters can be distributed at a low cost in rural areas. We plan to undertake the cost effectiveness of the technology developed so as to understand the cost involved in the filter developed and the health outcome (the reduction of bacteria can be correlated with number of water borne diseases being reported in an area).

**Acknowledgements** The authors thank the financial support from DST, New Delhi for the facilities provided to Sree Sankara College, Kalady under the DST-FIST program (No. 487/DST/FIST/15-16).

**Authors' Contributions** All the authors contributed equally to this work.

**Data Availability** The data that support the findings of this study are available from the corresponding author, [Dr. Sreekala M.S.], upon reasonable request.

## Declarations

**Ethics Approval and Consent to Participate** Not Applicable.

**Consent for Publication** Not Applicable.

**Conflict of Interest** The authors declare that they have no competing interests.

**Disclosure of potential Conflicting Interests** The authors declared no potential conflicts of interest concerning the research, authorship, and/or publication of this article.

**Research Involving Human Participants and/or Animals** Not Applicable.

**Informed Consent** Not Applicable.

## References

- Elimelech M (2006) The global challenge for adequate and safe water. *J Water Supply Res Technol - AQUA* 55(1):3–10
- Ashbolt NJ (2015) Microbial contamination of drinking water and human health from community water systems. *Curr Environ Health Rep*. <https://doi.org/10.1007/s40572-014-0037-5>
- Shannon MA, Bohn PW, Elimelech M et al (2008) Science and technology for water purification in the coming decades. *Nature* 452(7185):301–10
- Karimi-maleh H, Ayati A, Davoodi R, Tanhaei B (2021) Recent advances in using of chitosan-based adsorbents for removal of pharmaceutical contaminants: A review. *J Clean Prod* 291:125880. <https://doi.org/10.1016/j.jclepro.2021.125880>
- Orooji Y, Ghanbari M, Amiri O, Salavati-niasari M (2020) Facile fabrication of silver iodide / graphitic carbon nitride nanocomposites by notable photo-catalytic performance through sunlight and antimicrobial activity. *J Hazard Mater* 389:122079. <https://doi.org/10.1016/j.jhazmat.2020.122079>
- Orooji Y, Mohassel R, Amiri O, et al (2020) Gd<sub>2</sub>ZnMnO<sub>6</sub>/ZnO nanocomposites: Green sol-gel auto-combustion synthesis, characterization and photocatalytic degradation of different dye pollutants in water. *J Alloys Compd* 835:155240. <https://doi.org/10.1016/j.jallcom.2020.155240>
- Mehdizadeh P, Orooji Y, Amiri O, Salavati-niasari M (2020) Green synthesis using cherry and orange juice and characterization of TbFeO<sub>3</sub> ceramic nanostructures and their application as photocatalysts under UV light for removal of organic dyes in water. *J Clean Prod* 252:119765. <https://doi.org/10.1016/j.jclepro.2019.119765>
- Karimi-maleh H, Ranjbari S, Tanhaei B, et al (2021) Novel 1-butyl-3-methylimidazolium bromide impregnated chitosan hydrogel beads nanostructure as an efficient nanobio-adsorbent for cationic dye removal: Kinetic study. *Environ Res* 195:195. <https://doi.org/10.1016/j.envres.2021.110809>
- Sadeghi T, Ansarian Z, Darvishi R, et al (2020) Sonophotocatalytic activities of FeCuMg and CrCuMg LDHs: Influencing factors, antibacterial effects, and intermediate determination. *J Hazard Mater* 399:123062. <https://doi.org/10.1016/j.jhazmat.2020.123062>
- Fawell J, Nieuwenhuijsen MJ (2003) Contaminants in drinking water. *Br Med Bull* 68:199–20
- Sharma S, Bhattacharya A (2017) Drinking water contamination and treatment techniques. *Appl Water Sci*. <https://doi.org/10.1007/s13201-016-0455-7>
- Pandey PK, Kass PH, Soupir ML, et al (2014) Contamination of water resources by pathogenic bacteria. *AMB Express*. <https://doi.org/10.1186/s13568-014-0051-x>
- Vijaywada WAT, Vijayawada A, Dist K et al (2016) Water quality data 2016 | CPCB ENVIS For more information visit: <https://www.cpcbenvnis.nic.in>. 3581. Accessed 12/02/2021
- Annepu RK (2012) Sustainable solid waste management in India. Submitted in partial fulfillment of the requirements for the degree of Master of Science in Earth Resources Engineering Department of Earth and Environmental Engineering Fu Foundation School of Engineering and Applied Science Columbia University in the City of New York Sponsored by the Waste-to-Energy Research and Technology Council, Columbia University
- Edokpayi JN, Odiyo JO, Durowoju OS (2017) Impact of wastewater on surface water quality in developing countries: a case study of South Africa. In: *Water Quality*. <https://doi.org/10.5772/66561>
- Singh S, Kumar V, Romero R, Sharma K (2020) Applications of nanoparticles in wastewater treatment. *Nanobiotechnology in Bioformulations*. Nanotechnology in the Life Sciences. Springer, Cham, pp 349–379
- Brar SK, Verma M, Tyagi RD, Surampalli RY (2010) Engineered nanoparticles in wastewater and wastewater sludge – Evidence and impacts. *Waste Manag* 30:504–520. <https://doi.org/10.1016/j.wasman.2009.10.012>
- Bystrejskowska-piotrowska G, Golimowski J, Urban PL (2009) Nanoparticles: Their potential toxicity, waste and environmental management. *Waste Manag* 29:2587–2595. <https://doi.org/10.1016/j.wasman.2009.04.001>
- Salman M, Jahan S, Kanwal S, Mansoor F (2019) Recent advances in the application of silica nanostructures for highly improved water treatment: a review. *Environ Sci Pollut Res* 26(21):21065–2108
- Brigante M, Pecini E, Avena M (2016) Magnetic mesoporous silica for water remediation: Synthesis, characterization and application as adsorbent of molecules and ions of environmental concern. *Microporous Mesoporous Mater* 230:1–10. <https://doi.org/10.1016/j.micromeso.2016.04.032>
- Alotaibi KM, Shiels L, Lacaze L, et al (2016) Iron supported on bioinspired green silica for water remediation. *Chem Sci* 8:567–576. <https://doi.org/10.1039/c6sc02937j>
- Crini G (2005) Recent developments in polysaccharide-based materials used as adsorbents in wastewater treatment. *Prog Polym Sci* 30:38–70. <https://doi.org/10.1016/j.progpolymsci.2004.11.002>
- Crini G (2006) Non-conventional low-cost adsorbents for dye removal: A review. *Bioresour Technol* 97:1061–1085. <https://doi.org/10.1016/j.biortech.2005.05.001>
- Etcheverry M, Cappa V, Trelles J, Zanini G (2017) Montmorillonite-alginate beads: Natural mineral and biopolymers based sorbent of paraquat herbicides. *J Environ Chem Eng* 5:5868–5875. <https://doi.org/10.1016/j.jece.2017.11.018>
- Dongre RS, Sadasivuni KK, Deshmukh K, et al (2019) Natural polymer based composite membranes for water purification: a review. *Polym Plast Technol Mater* 58:1
- Shim J, Lim JM, Shea PJ, Oh BT (2014) Simultaneous removal of phenol, Cu and Cd from water with corn cob silica-alginate beads. *J Hazard Mater* 272:129–136. <https://doi.org/10.1016/j.jhazmat.2014.03.010>
- Baek S, Joo SH, Toborek M (2019) Treatment of antibiotic-resistant bacteria by encapsulation of ZnO nanoparticles in an

- alginate biopolymer: Insights into treatment mechanisms. Elsevier B.V., Amsterdam
28. Wang F, Lu X, Li XY (2016) Selective removals of heavy metals (Pb<sup>2+</sup>, Cu<sup>2+</sup>, and Cd<sup>2+</sup>) from wastewater by gelation with alginate for effective metal recovery. *J Hazard Mater* 308:75–83. <https://doi.org/10.1016/j.jhazmat.2016.01.021>
  29. Kuang Y, Du J, Zhou R, et al (2015) Calcium alginate encapsulated Ni/Fe nanoparticles beads for simultaneous removal of Cu (II) and monochlorobenzene. *J Colloid Interface Sci* 447:85–91. <https://doi.org/10.1016/j.jcis.2015.01.080>
  30. Ociński D, Jacukowicz-Sobala I, Kociołek-Balawejder E (2016) Alginate beads containing water treatment residuals for arsenic removal from water—formation and adsorption studies. *Environ Sci Pollut Res* 23:24527–24539. <https://doi.org/10.1007/s11356-016-6768-0>
  31. Lin S, Huang R, Cheng Y, et al (2013) Silver nanoparticle-alginate composite beads for point-of-use drinking water disinfection. *Water Res* 47:3959–3965. <https://doi.org/10.1016/j.watres.2012.09.005>
  32. Shim J, Kumar M, Mukherjee S, Goswami R (2019) Sustainable removal of pernicious arsenic and cadmium by a novel composite of MnO<sub>2</sub> impregnated alginate beads: A cost-effective approach for wastewater treatment. *J Environ Manage* 234:8–20. <https://doi.org/10.1016/j.jenvman.2018.12.084>
  33. World Health Organisation (2017) Potable reuse: guidance for producing safe drinking-water. World Health Organization. <https://apps.who.int/iris/handle/10665/258715>. License: CC BY-NC-SA 3.0 IGO
  34. Valgas C, De Souza SM, Smânia EFA, Smânia A (2007) Screening methods to determine antibacterial activity of natural products. *Brazilian J Microbiol* 38:369–380. <https://doi.org/10.1590/S1517-83822007000200034>
  35. Nelson MT, Labudde RA, Tomasino SF, Pines RM (2013) Comparison of 3MTM petrifilm™ Aerobic Count plates to standard plating methodology for use with AOAC antimicrobial efficacy methods 955. 14 955. 15, 964.02, and 966.04 as an alternative enumeration procedure: Collaborative study. *J AOAC Int*. <https://doi.org/10.5740/jaoacint.12-469>
  36. Carmona VB, Oliveira RM, Silva WTL, et al (2013) Nanosilica from rice husk: Extraction and characterization. *Ind Crop Prod* 43:291–296. <https://doi.org/10.1016/j.indcrop.2012.06.050>
  37. Mor S, Manchanda CK, Kansal SK, Ravindra K (2017) Nanosilica extraction from processed agricultural residue using green technology. *J Clean Prod* 143:1284–1290. <https://doi.org/10.1016/j.jclepro.2016.11.142>
  38. Yuvakkumar R, Elango V, Rajendran V, Kannan N (2014) High-purity nano silica powder from rice husk using a simple chemical method. 8080:. <https://doi.org/10.1080/17458080.2012.656709>
  39. Rafiee E, Shahebrahimi S, Feyzi M, Shaterzadeh M (2012) Optimization of synthesis and characterization of nanosilica produced from rice husk (a common waste material). *Int Nano Lett* 21 2:1–8. <https://doi.org/10.1186/2228-5326-2-29>
  40. Hassan AF, Abdelghny AM, Elhadidy H, Youssef AM (2013) Synthesis and characterization of high surface area nanosilica from rice husk ash by surfactant-free sol–gel method. *J Sol-Gel Sci Technol* 693 69:465–472. <https://doi.org/10.1007/S10971-013-3245-9>
  41. Wang W, Martin JC, Fan X et al (2012) Silica nanoparticles and frameworks from rice husk biomass. *ACS Appl Mater Interfaces* 4:977–981. <https://doi.org/10.1021/AM201619U>
  42. Nguyen TT, Ma HT, Avti P, et al (2019) Adsorptive removal of iron using SiO<sub>2</sub> nanoparticles extracted from rice husk ash. *J Anal Methods Chem* 2019. <https://doi.org/10.1155/2019/6210240>
  43. Salama A, Diab MA, Abou-Zeid RE, et al (2018) Crosslinked alginate/silica/zinc oxide nanocomposite: A sustainable material with antibacterial properties. *Compos Commun* 7:7–11. <https://doi.org/10.1016/j.coco.2017.11.006>
  44. Mukharjee BB, Barai S V (2015) Characteristics of sustainable concrete incorporating recycled coarse aggregates and colloidal nano-silica. *Adv Concr Constr* 3:187–202. <https://doi.org/10.12989/acc.2015.3.3.187>
  45. Dung PD, Ngoc LS, Duy NN et al (2016) Effect of nanosilica from rice husk on the growth enhancement of chili plant (*Capsicum frutescens* L.). *Vietnam J Sci Technol* 54:607. <https://doi.org/10.15625/0866-708x/54/5/7034>
  46. Pannier A, Soltmann U, Soltmann B, et al (2014) Alginate/silica hybrid materials for immobilization of green microalgae *Chlorella vulgaris* for cell-based sensor arrays. *J Mater Chem B* 2:7896–7909. <https://doi.org/10.1039/c4tb00944d>
  47. Kuskutham B, Prasertgul J, Srinun P (2014) Morphology and property of calcium silicate encapsulated with alginate beads. *Silicon* 6:191–197. <https://doi.org/10.1007/s12633-013-9173-z>
  48. Rehbein P, Raguz N, Schwalbe H (2019) Evaluating mechanical properties of silica-coated alginate beads for immobilized biocatalysis. *Biochem Eng J* 141:225–231. <https://doi.org/10.1016/j.bej.2018.10.028>
  49. Gok C, Aytas S (2009) Biosorption of uranium(VI) from aqueous solution using calcium alginate beads. *J Hazard Mater* 168:369–375. <https://doi.org/10.1016/j.jhazmat.2009.02.063>
  50. Roosen J, Pype J, Binnemans K, Mullens S (2015) Shaping of alginate – Silica hybrid materials into microspheres through vibrating-nozzle technology and their use for the recovery of neodymium from aqueous solutions. <https://doi.org/10.1021/acs.iecr.5b03494>
  51. Sharma SK, Sharma AR, Pamidimarri SD, Gaur J, Singh BP, Sekar S, ... Lee SS (2019) Bacterial compatibility / toxicity of biogenic silica (b-SiO<sub>2</sub>) Nanoparticles synthesized from biomass. *Nanomaterials* 9:1440. <https://doi.org/10.3390/nano9101440>
  52. Capeletti LB, De Oliveira LF, Gonçalves KDA, et al (2014) Tailored silica-antibiotic nanoparticles: Overcoming bacterial resistance with low cytotoxicity. *Langmuir* 30:7456–7464. <https://doi.org/10.1021/la4046435>
  53. Alshatwi AA, Athinarayanan J, Periasamy VS (2015) Biocompatibility assessment of rice husk-derived biogenic silica nanoparticles for biomedical applications. *Mater Sci Eng C* 47:8–16. <https://doi.org/10.1016/j.msec.2014.11.005>
  54. De Oliveira LF, De Almeida Gonçalves K, Boreli FH, et al (2012) Mechanism of interaction between colloids and bacteria as evidenced by tailored silica-lysozyme composites. *J Mater Chem* 22:22851–22858. <https://doi.org/10.1039/c2jm34899c>
  55. Lin YS, Haynes CL (2010) Impacts of mesoporous silica nanoparticle size, pore ordering, and pore integrity on hemolytic activity. *J Am Chem Soc* 132:4834–4842
  56. Nel AE, Mädler L, Velegol D, et al (2009) Understanding bio-physicochemical interactions at the nano-bio interface. *Nat Mater* 8:543–557. <https://doi.org/10.1038/nmat2442>
  57. Slowing II, Wu CW, Vivero-Escoto JL, Lin VSY (2009) Mesoporous silica nanoparticles for reducing hemolytic activity towards mammalian red blood cells. *Small* 5:57–62. <https://doi.org/10.1002/sml.200800926>
  58. Deo SS, Gidde MR (2019) Managing pollution impacted potable groundwater in rural area of eastern pune metropolitan region: disinfection by common plants. 9869–9875. <https://doi.org/10.35940/ijrte.D9153.118419>
  59. Tarroza AVZ, Catsao K V, Ramos MA et al (2019) Utilization of hydrated petrifilm coupled with filtration in the detection and enumeration of *escherichia coli* in water samples. *Philipp J Sci* 148:395–399
  60. Tufenkji N, Elimelech M (2004) Correlation equation for predicting single-collector efficiency in physicochemical filtration in saturated porous media. *Environ Sci Technol* 38:529–536. <https://doi.org/10.1021/es034049r>

**Publisher's Note** Springer Nature remains neutral with regard to jurisdictional claims in published maps and institutional affiliations.